Quaternary Science Reviews 127 (2015) 61–72

Contents lists available at ScienceDirect

Quaternary Science Reviews

journal homepage: www.elsevier.com/locate/quascirev

Impacts of cave air ventilation and in-cave prior calcite precipitation on Golgotha Cave dripwater chemistry, southwest Australia

Pauline C. Treble [a, *], Ian J. Fairchild [b], Alan Griffiths [a], Andy Baker [c], Karina T. Meredith [a], Anne Wood [d], Elizabeth McGuire [d]

[a] Institute for Environmental Research, Australian Nuclear Science and Technology Organisation, Lucas Heights, NSW, Australia
[b] School of Geography, Earth and Environmental Sciences, University of Birmingham, Edgbaston, Birmingham, UK
[c] Connected Waters Initiative Research Centre, University of New South Wales Australia, Sydney, NSW, Australia
[d] Department of Parks and Wildlife, 14 Queen St, Busselton, WA, Australia

ARTICLE INFO

Article history:
Received 1 March 2015
Received in revised form
26 May 2015
Accepted 1 June 2015
Available online 23 June 2015

Keywords:
Speleothem
Cave ventilation
Cave monitoring
Dripwater
Prior calcite precipitation
Fire

ABSTRACT

Speleothem trace element chemistry is an important component of multi-proxy records of environmental change but a thorough understanding of hydrochemical processes is essential for its interpretation. We present a dripwater chemistry dataset (PCO_2, alkalinity, Ca, SI_{cc}, Mg and Sr) from an eight-year monitoring study from Golgotha Cave, building on a previous study of hydrology and dripwater oxygen isotopes (Treble et al., 2013). Golgotha Cave is developed in Quaternary aeolianite and located in a forested catchment in the Mediterranean-type climate of southwest Western Australia. All dripwaters from each of the five monitored sites become supersaturated with respect to calcite during most of the year when cave ventilation lowers PCO_2 in cave air. In this winter ventilation mode, prior calcite precipitation (PCP) signals of increased Mg/Ca and Sr/Ca in dripwater are attributed to stalactite deposition. A fast-dripping site displays less-evolved carbonate chemistry, implying minimal stalactite growth, phenomena which are attributed to minimal degassing because of the short drip interval (30 s).

We employ hydrochemical mass-balance modelling techniques to quantitatively investigate the impact of PCP and CO_2 degassing on our dripwater. Initially, we reverse-modelled dripwater solutions to demonstrate that PCP is dominating the dripwater chemistry at our low-flow site and predict that PCP becomes enhanced in underlying stalagmites. Secondly, we forward-modelled the ranges of solution Mg/Ca variation that potentially can be caused by degassing and calcite precipitation to serve as a guide to interpreting the resulting stalagmite chemistry. We predict that stalagmite trace element data from our high-flow sites will reflect trends in original dripwater solutes, preserving information on biogeochemical fluxes within our system. By contrast, stalagmites from our low-flow sites will be dominated by PCP effects driven by cave ventilation. Our poorly karstified system allows us to highlight and quantify these in-cave (PCP) processes, which are otherwise masked at sites where karstification is more developed and hydrogeology is more complex. Our modelling also shows enhanced CO_2 source production in the unsaturated zone that is attributed to deeply-rooted vegetation and increasing bioproductivity which we link to forest recovery after fires impacted our site during 2006 CE.

1. Introduction

Speleothem trace elements are derived from minor and trace concentrations of solutes in cave dripwater. These solutes may be derived from incoming meteoric precipitation, dust, sea spray and soil/bedrock leaching (Baker et al., 2000; Musgrove and Banner, 2004; Fairchild and Treble, 2009; Hartland et al., 2012; Baldini et al., 2015) and their subsequent concentrations in dripwater modified by biogeochemical processes in the unsaturated zone (e.g. nutrient cycling and organic matter flux; Hartland et al., 2012; Wynn et al., 2013) and karst hydrological flowpaths (e.g. mixing and dilution; Tooth and Fairchild, 2003). The construction of high-resolution (sub-annual or better) speleothem trace element records by in situ methods (laser–ablation inductively coupled plasma mass spectrometry, ion microprobe and synchrotron X-ray fluorescence) is becoming a relatively common and straightforward

* Corresponding author. PMB 2001 Kirrawee DC NSW 2232, Australia.
E-mail address: pauline.treble@ansto.gov.au (P.C. Treble).

http://dx.doi.org/10.1016/j.quascirev.2015.06.001
0277-3791/

process. As such, they are an important component of multi-proxy information used for paleo-environmental interpretation (e.g. Treble et al., 2003; Frisia et al., 2005; Fairchild et al., 2006; McMillan et al., 2005; Johnson et al., 2006; Cruz et al., 2007; Hori et al., 2014; Orland et al., 2014; Rutlidge et al., 2014; Wynn et al., 2014).

Speleothem formation and the incorporation of minor and trace elements from dripwater into speleothem calcite are broadly well-understood (Fairchild and Baker, 2012). Calcite precipitation from dripwaters leading to stalagmite formation may be generally described as follows: i) the initial stage of dissolved CO_2-degassing as dripwater emerges from the cave ceiling, ii) equilibration of the dripwater with cave PCO_2 via the hydration of CO_2; and iii) calcite precipitation. This evolution of chemical species is predominantly characterised by a reduction in dripwater PCO_2 during equilibration and a reduction in both [Ca^{2+}] and [HCO_3^-] during precipitation driven by consumption of these ions (Hansen et al., 2013). Minor and trace elements present in dripwater may become incorporated into the growing speleothem (Gascoyne, 1983; Huang and Fairchild, 2001; Fairchild and Treble, 2009; Day and Henderson, 2013). Those that readily substitute for Ca in the carbonate crystal lattice, such as Mg and Sr, are known to behave in a predictable manner (see Fairchild and Treble, 2009). Their uptake has been determined experimentally, including for cave-analogue conditions (Huang and Fairchild, 2001; Day and Henderson, 2013), and is defined by the partition coefficient, K, (Equation (1)). Using Mg as an example:

$$K_{Mg} = [Mg/Ca]_{calcite} \Big/ [Mg/Ca]_{fluid} \quad (1)$$

The origin of trace elements in cave dripwaters may be constrained by the chemical characterisation of end-members (bedrock, dust, etc) providing a basis for interpreting the speleothem trace element record (e.g. Goede et al., 1998; Musgrove and Banner, 2004; Tremaine and Froelich, 2013). However, the most appropriate interpretation may be more challenging, owing to the subsequent water/rock interactions occurring along individual water flowpaths associated with hydrological routing (Tooth and Fairchild, 2003; Baldini et al., 2006; McDonald and Drysdale, 2007).

A common process that can dominate the ultimate concentrations of these ions in dripwater is prior calcite precipitation (PCP). PCP is defined as the calcite precipitated from a solution before it reaches the stalagmite. This is caused by the fluid equilibrating with lower PCO_2 conditions along its flowpath in the unsaturated zone (Fairchild et al., 2000). PCP is commonly diagnosed using speleothem Mg/Ca or Sr/Ca, as $K << 1$ for these ions results in these ratios becoming higher in the precipitating fluid. Since water-residence time along a flowpath in the unsaturated zone typically increases during periods of lower recharge, evidence for enhanced PCP in a speleothem record has become a useful and common diagnostic for recharge variations (e.g. Johnson et al., 2006; Karmann et al., 2007; Sinclair et al., 2012), particularly drought periods (McDonald et al., 2004).

Karst CO_2 gradients are also an important driver in the PCP process. Cave CO_2 concentration is governed by a balance between CO_2 production by microbial and root respiration in the overlying soil and vadose zone, cave biological activity, and the loss of CO_2 from the cave to the atmosphere (Fairchild and Baker, 2012). It is now recognised that many caves experience a seasonal build-up of CO_2 concentration that is not primarily related to CO_2 production but controlled by seasonal contrasts in temperature and/or pressure gradients promoting or restricting cave ventilation. The more typical situations are temperature-driven buoyancy flows promoting stronger ventilation in cooler months and high cave PCO_2 in warmer months (Spötl et al., 2005; Frisia et al., 2011; Miorandi et al., 2010; Kowalczk and Froelich, 2010; Lambert and Aharon, 2011). Ventilation-driven changes in cave PCO_2 has been shown to drive seasonal variability in PCP (Wong et al., 2011).

Cave monitoring is a useful exercise for understanding processes in a particular karst system including PCP (e.g. Genty and Deflandre, 1998; Miorandi et al., 2010; Pape et al., 2010; Wong et al., 2011; Riechelmann et al., 2013; Tremaine and Froelich, 2013). However, clearly identifying PCP via cave monitoring has been confounded by karst systems with complex hydrogeology, with particularly marked variations in water routing and storage (e.g. Tooth and Fairchild, 2003). Given these constraints, it would clearly be advantageous to analyse data from a cave with relatively simple hydrogeology when investigating PCP in cave environments.

Here, we examine the impacts of in-cave processes (drip rate, cave CO_2 and ventilation) on a long dripwater dataset (2005–2014 CE) from Golgotha Cave, SW Western Australia. Golgotha Cave has a relatively simple hydrogeology and constant drip rates, identified previously using dripwater isotopes and a karst hydrology model (Treble et al., 2013). Both of these features are owing to the predominance of matrix flow pathways in the young dune limestone in which Golgotha Cave is developed. In the current study, we focus on the dripwater carbonate species and cave CO_2 concentrations, and examine the potential for in-cave processes to modifying the dripwater solute chemistry. In a forthcoming paper, we will examine the processes responsible for the concentrations of these solutes in our dripwater and examine the environmental signals contained in their long-term trends.

2. Site description

Golgotha Cave (36.10°S 115.05°E) is located in the Leeuwin-Naturaliste National Park and is developed in the Spearwood System of the Tamala Limestone, a coastal belt of dune limestone that extends along >1000 km of the SW Western Australia coastline (Fig. 1A). The Spearwood System comprises medium-to coarse-grained Quaternary aeolian calcarenite mantled by weathered siliceous dune sands (Hall and Marnham, 2002). Golgotha Cave has only one known entrance, which faces east (Fig. 1B). The entrance is relatively large, approximately 350 m^2, although the cross-sectional area of the cave narrows by 50% approximately 20 m inside the entrance, at the point where the floor steeply rises by 10 m towards the ceiling (Fig. 1C). Here there is a noticeable change to higher humidity and reduced air movement and quality. Thus while the relatively large entrance facilitates air exchange, the interior atmosphere is more stable. Only a narrow range of temperatures between 14.5 and 15.0 °C have been recorded and the relative humidity has consistently exceeded 90% when determined on cave visits at different times of the year (Treble et al., unpublished data). Access to the cave is restricted by an open-grid wooden gate at the entrance.

Golgotha Cave lies in the winter rainfall zone of southern Australia: >75% of annual rainfall (1113 ± 165 mm) falls between May and September and mean annual evapotranspiration rates are estimated to be 730 ± 42 mm calculated using the climatological mean 1985–2014 (Raupach et al., 2009, 2012). An extensive eucalypt forest covers Golgotha Cave and the surrounding area. These tall trees have deep roots that can penetrate tens of metres deep in the Tamala Limestone and may be associated with the formation of discrete flow pathways above the cave (Treble et al., 2013). The area above and around Golgotha Cave has been impacted by fire, most recently in 2006 CE, and prior to this in 1992 and 1998 CE (DPaW, 2012).

Our five long-term monitoring sites are located in two areas of Golgotha Cave with contrasting dune facies as described in Treble et al. (2013) (Fig. 1B–C). The first area, approximately 60 m into the cave and housing sites 1A and 1B, has a 4 m tall ceiling with sites 1A and 1B receiving water from individual soda-straw stalactites that are 0.5 m apart. The second area housing sites 2A, 2B

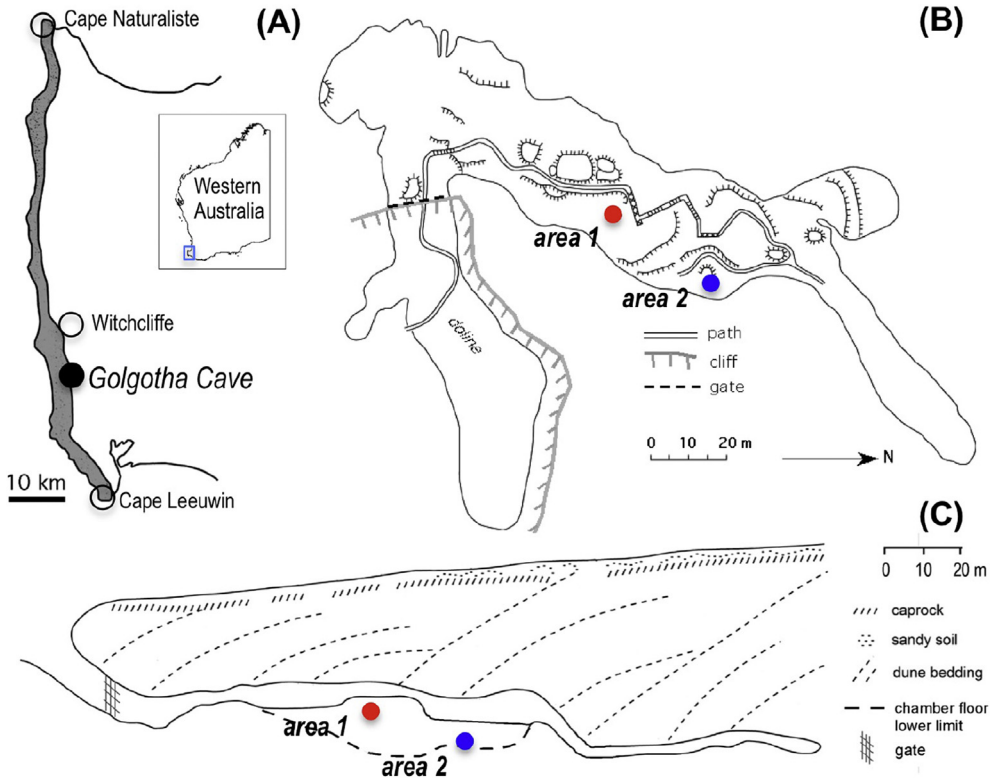

Fig. 1. A–C: (A) Location figure for Golgotha Cave, SW Western Australia with grey shading indicating dune limestone, (B) plain view of Golgotha Cave; (C) longitudinal section of Golgotha Cave relative to the main path through the cave. Red and blue dots indicate dripwater sampling areas (area 1: sites 1A and 1B; area 2: sites 2A, 2B and 2E). Figures A and B adapted from Treble et al. (2013). (For interpretation of the references to colour in this figure legend, the reader is referred to the web version of this article.)

and 2E is approximately 90 m into the cave in a much larger chamber with a taller ceiling than at site 1, but which slopes steeply downwards towards our collection sites, although the absolute ceiling elevation is overall lower and the overburden higher compared with site 1 (Fig. 1C). Stalactites tend to be shorter, more isolated and populated by relatively fewer soda-straw stalactites at sampling area 2. Sites 2A, 2B and 2E are fed by soda-straw stalactites, although the stalactite feeding site 2B has thickened via externally-deposited calcite also. The ceiling is too high at site 2B to confirm if water is currently flowing over the stalactite exterior, but at all other drip sites, it appears from our field observations that dripwater is derived from water flowing inside the soda-straw, rather than on the exterior. A detailed description of the ceiling and stalactite morphology, as well as a geostatistically-based interpretation of the infiltration to these sites will appear in a forthcoming article (Mahmud et al., in review).

Data from the five long-term monitoring sites indicate that drip rates were relatively constant at each site in the seven years reported in Treble et al. (2013) despite the highly seasonal winter precipitation and summer soil moisture deficit. This is typical of infiltration into Golgotha Cave, confirmed by the more recent deployment of 28 automated drip loggers in 2012 CE (Treble et al., unpublished data). We infer that water movement to Golgotha Cave occurs almost solely via a matrix flow mechanism facilitated by the high primary porosity of the host rock at this site (Treble et al., 2013). Using dripwater oxygen isotopes, Treble et al. (2013) recognised that these matrix-flow pathways could be spatially distinct and preferential. For example, site 2E (referred to as our high-flow site) is located within a zone of higher dripwater flux interpreted to arise from seepage from a relatively large and discrete water store (Treble et al., 2013). Site 2B is on the periphery of this zone (5 m from 2E) whilst site 2A is several metres further away; dripwater fluxes are lower here, but flux rates are comparable to the majority of drips elsewhere in Golgotha Cave. At the beginning of the monitoring period, the drip rate at site 2B was higher and Treble et al. (2013) interpreted that 2B was receiving overflow from the larger water store (associated with site 2E) but these fluxes apparently ceased in February 2007 whereupon site 2B reverted to low constant discharge similar to site 2A.

3. Methods

3.1. Cave and soil CO_2

Cave CO_2 was measured at sites 1A-1B from January 2008, initially by manual spot sampling, and from March 2009 onwards, continuously logged, at 30 min intervals, via a Vaisala GM70/GMP222 (manufacturer's precision ±1%) with an overlapping interval of 9 months. Manual spot sampling was conducted by opening a 12 ml pre-evacuated glass tube, which was flushed three times with cave air using a 20 ml syringe, before re-sealing the tube with a rubber stopper. CO_2 concentrations were determined by an infra-red gas analyser at the Australian National University with a precision of ±0.5% (1 s.e., n = 10). Periods of missing CO_2 data are owing to either battery malfunction or the logger requiring removal for factory calibration. Soil CO_2 was measured using a Draeger device (manufacturer's precision ±5%) and soil probe described in Miotke (1974) at an approximate depth of 40 cm in approximately the same location, during cave visits from May to December 2008.

3.2. Dripwater analyses

Cave dripwaters accumulated in 1 L high-density polyethylene (HDPE) collection vessels, fitted with funnels, with overflow

permitted via a 5 mm hole punched below the bottle neck. At intervals of between 4 and 6 weeks, pH, EC and temperature of these bulk water samples were measured using a hand-held TPH1-MyronL TechPro II meter, calibrated using fresh buffer solutions (pH 7 and 10) equilibrated to cave temperature. The remaining water was collected for transport out of the cave and the vessel emptied. Additionally, in situ monitoring of dripwater pH was carried out during cave visits in September 2008 using a 3 mm micro electrode (Orion PerpHecT ROSS combination) immersed inside a custom-built small volume flow-through cell (0.4 ml) positioned directly beneath our high (2E) and low-flow (1A) drip sites. The micro-electrodes were calibrated using the same buffer solutions as above, and both electrodes produced pH measurements that agreed within the manufacturer's precision.

Outside of the cave, total alkalinity (as mg/l $CaCO_3$) was determined by acid-base titration (1.6 N H_2SO_4) to a methyl-orange endpoint using a Hach digital titrator (model 16900) on duplicate 100 ml sub-samples of the bulk water within 1 h of water collection. The remaining water was filtered with 0.45 μm mixed-cellulose filters into two 50 ml polypropylene bottles and refrigerated below 5 °C until analysis at ANSTO. One sub-sample was used for anion concentrations (Cl and SO_4) determined using a Dionex DX-600 ion chromatograph with self-regenerating suppressor while the other was acidified to 2% HNO_3 in the collection bottle and used for cation concentrations (Ca, K, Mg, Na, Si and Sr) using a Thermo Fisher inductively coupled plasma-atomic emission spectroscopy (ICP-AES) ICAP7600. An internal standard with concentrations approximating the cave waters was included in each cation batch to check for between-run reproducibility. Saturation indices for calcite (SIcc) and PCO_2 were calculated using the WATEQ4F thermodynamic database in PHREEQC 2.4.2 program (Parkhurst and Appelo, 1999). Seven samples at site 1A had K concentrations between 4 and 450 times higher than the mean. These occurred between May 2009 and January 2010 during the period in which the micro-pH electrodes were installed at this site and as such, we suspect that they were contaminated by KCl from the electrode storage solution. We discarded the K data for these and a correction was made on the affected Cl data by subtracting the calculated contribution of Cl from the KCl, assuming that the K in the affected data was overwhelming due to contamination. Charge balance errors were checked for samples with a full suite of major ion chemistry and 89% of our data were within ±5% and the remaining within ±10%.

3.3. Modelling dripwaters

Cave environment datasets are complemented by a modelling approach to elucidate their meaning (Fairchild and Baker, 2012, p. 180–186). Broadly three approaches can be envisaged to trace element modelling:

a) conceptual, grey-box modelling where a parameterized approach is used to demonstrate the possible impact of controlling processes, e.g. the roles of rainfall and PCO_2 variations on Mg and Sr chemistry in speleothems in the study of Wong et al. (2011).
b) a mass-balance, equilibrium thermodynamic approach, using the well-characterized carbonate system parameters encoded in chemical speciation models and estimated values of water-calcite partition coefficients (e.g. Fairchild et al., 2000; Mattey et al., 2010; Tremaine and Froelich, 2013). A similar mass-balance philosophy underpins the carbon isotope studies of Spötl et al. (2005) and Frisia et al. (2011) and such an approach can include mixing of defined end-members as well as evolution of solutions.
c) a combination of the mass-balance approach with kinetic models. For example, Fairchild et al. (2000) modelled the consequences of competitive dissolution of dolomite and calcite on karst water chemistry. The most complete study of this kind is the I-STAL model of Stoll et al. (2012) which incorporates mathematical functions for hydrological controls on water–rock interactions during weathering, crystal growth rate in relation to solution supersaturation and growth rate controls on partition coefficients.

In this paper, we take a pure mass-balance approach, using the standard assumptions in the above literature. We do not explicitly consider the weathering reactions here, but in a future paper will discuss the contributions made by carbonate bedrock, biomass and atmospheric salts. We model dripwaters supersaturated for calcite, implying degassing of CO_2 from a previously saturated solution. Hence, the starting point we consider, based on the fast dissolution kinetics of calcite, is a solution in equilibrium with calcite, whose Ca content reflects the highest PCO_2 encountered in the soil and epikarst. The data arrays in the hydrologically simple case presented by Golgotha Cave do not require us to consider mixing of fluids from different aquifer compartments. The supersaturated solution will evolve in composition by precipitation of calcite which has a much lower Mg/Ca and Sr/Ca than the precipitating solution and hence the solution with the lowest values of these ratios (and the highest Ca) is likely to be closest to the original solution before calcite precipitation. Standard calculations (Fairchild et al., 2000; Tremaine and Froelich, 2013) are used to produce PCP trendlines for our dripwaters, as outlined here for Mg/Ca using molar concentrations:

i) starting with the highest measured Ca concentration (Ca_0) for each site, we set-up an array of decreasing Ca concentrations i.e. Ca_0, Ca_1, Ca_2, …, etc;
ii) using the measured Mg/Ca ratio for Ca_0 i.e. $Mg/Ca_{(aq)0}$, we calculate the Mg/Ca of calcite precipitating from this solution, $Mg/Ca_{(cc)0} = Mg/Ca_{(aq)0} \times K_{Mg}$;
iii) we calculated the small amount of Mg lost from solution as $Mg_{(cc)0} = Mg/Ca_{(cc)0} \times (Ca_0 - Ca_1)$;
iv) the above is used to calculate the Mg concentration of the remaining solution, $Mg_{(aq)1} = Mg_{(cc)0} - Mg_{(aq)0}$, and hence generate $Mg/Ca_{(aq)1}$ and further values as an iterative process.

This approach may be used to estimate a theoretical slope of Sr/Mg (depending on partition coefficients used) to diagnose PCP in dripwaters (cf. Sinclair et al., 2012) that takes into account a given starting composition. Partition coefficients adopted here are: $K_{Mg} = 0.019$ for Mg (Huang and Fairchild, 2001) and $K_{Sr} = 0.1$, the latter as a mid-range estimate for Sr from Fig. 8.11 in Fairchild and Baker (2012).

Reverse and forward mass-balance modelling experiments on carbonate system behaviour were undertaken using the chemical speciation software MIX4 (Fairchild and Baker, 2012, p. 150), an operationally convenient simplified relative of the program PHREEQ which yields the same results for saturation index and PCO_2 within 0.01–0.02 using the accepted solubility product for calcite of $10^{-8.43}$ at a cave temperature of 15 °C.

4. Results

4.1. Cave CO_2 and seasonal ventilation

The CO_2 concentration in cave air has a strong seasonal cycle with highest values during the warmer months and lowest values,

just above typical atmospheric concentrations, during the cooler months (Fig. 2). For caves like Golgotha, with a single entrance, buoyancy-driven ventilation is the most likely process behind the ten-fold seasonal variation in CO_2 (Fairchild and Baker, 2012).

To show that buoyancy-driven flows actually are dominant in Golgotha Cave, we examined the relationship between variations in outside air temperature, the main cause of a buoyancy force, and cave CO_2. Evidence that such a relationship exists is shown in Fig. 3, where an outside temperature of ~15 °C separates the high-CO_2 from low-CO_2 modes. This threshold temperature is within the range of our cave air temperature measurements (14.5–15.0 °C) and close to the external mean air temperature (15.9 °C for 1999–2013; Bureau of Meteorology, 2014), which we have taken to be equal to the temperature measured at the nearby Witchcliffe weather station (Fig. 1A). The CO_2 response is not instantaneous, so to clearly visualise this effect the external air temperature has been smoothed and lagged with an exponentially weighted moving average (EWMA) filter, using a span of 48 h.

4.2. Dripwater chemistry

Time series of P-ET, drip rate, PCO_2, Ca, alkalinity and SI_{CC} are shown in Fig. 2. Dripwater PCO_2, Ca, alkalinity, SI_{CC} are dominated by strong seasonality at all sites except at our high-flow site, 2E, which has much less variability (Fig. 2). Our low-flow sites are following the seasonal cycle of cave air PCO_2 and are much closer to being completely degassed and in equilibrium with cave air, in contrast to the high-flow site (2E) where higher dripwater PCO_2 values are typically maintained when cave CO_2 lowers (Fig. 2). All sites become supersaturated with respect to calcite (SIcc) indicating that the potential for calcite precipitation increases from April until October/November when cave air PCO_2 falls, although

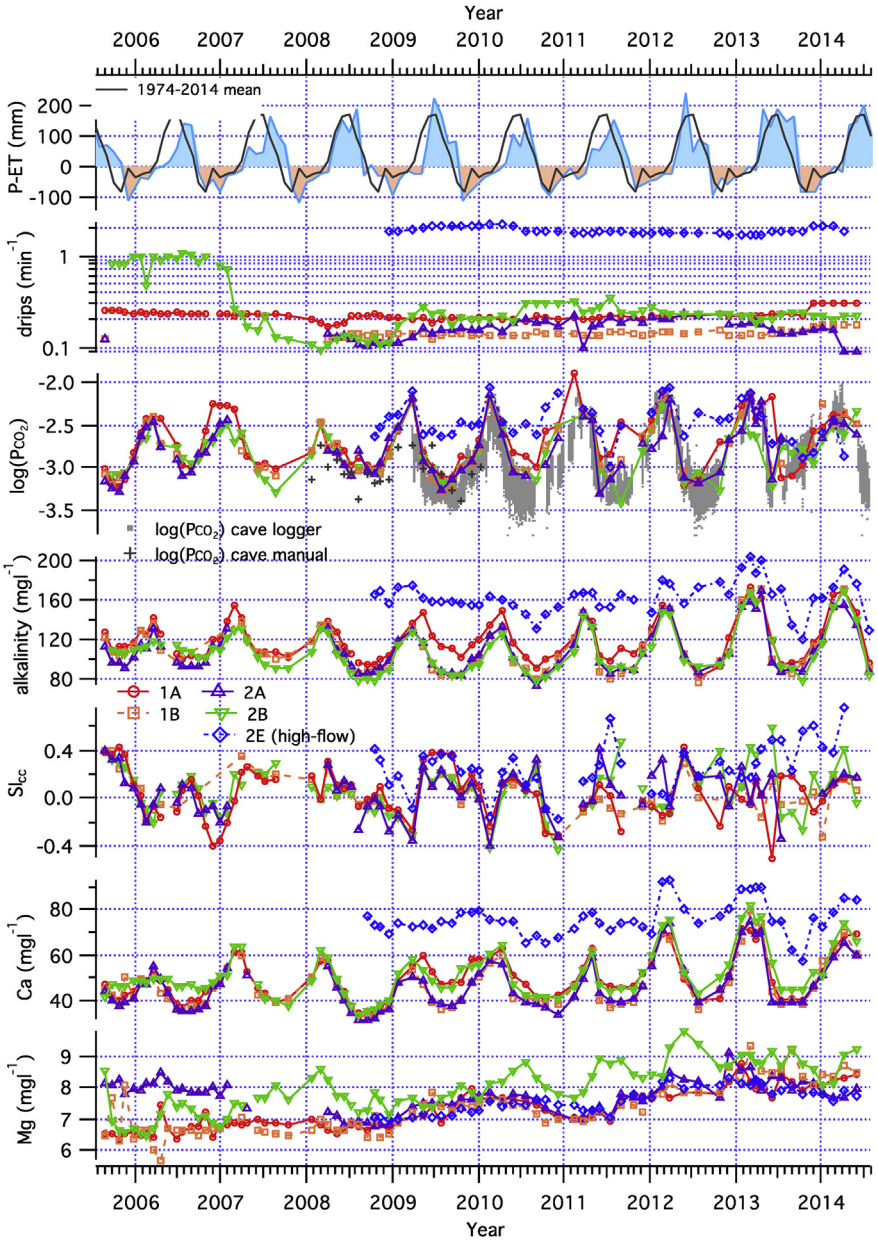

Fig. 2. Time series of P-ET, drip rate, PCO_2, alkalinity, SI_{CC}, Ca, and Mg data at each of the drip sites for Golgotha Cave. Monthly P-ET values are the blue line superimposed over shading representing the 1970–2014 P-ET mean. P-ET is calculated using precipitation minus modelled evapotranspiration (parameter 'FEW') extracted at our location from the AWAP database (Raupach et al., 2009, 2012). (For interpretation of the references to colour in this figure legend, the reader is referred to the web version of this article.)

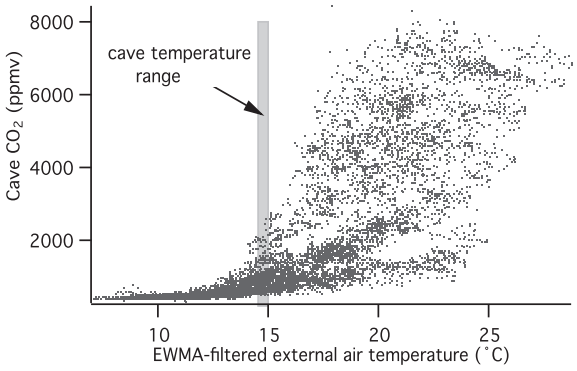

Fig. 3. In situ hourly measured cave air CO_2 versus hourly external air temperature. A vertical grey bar indicates the range of internal cave air temperatures measured near site 1. Air temperature is filtered using an EWMA with a span of 48 h. The EWMA is defined as: $y_i = (1 - \alpha)y_{i-1} + \alpha x_i$, where y_i is the i th output and x_i the i th input. The parameter, α, which determines the degree of smoothing is related to the span, s, via $\alpha = 2/(s + 1)$.

SIcc values are higher overall for the high-flow site owing to higher Ca and alkalinity. Mean Ca concentrations are also 20% higher, with reduced seasonality, for site 2B during the period of higher drip rates that occurred prior to February 2007. Low-flow sites exhibit periods where calcite is undersaturated. Thus calcite deposition is more likely to be uninterrupted at the high-flow site whilst it may be seasonally limited at the low-flow sites.

A potential uncertainty with field collection of cave dripwaters is the degassing of dripwater CO_2 and precipitation of $CaCO_3$ in our collection vessels during the 4–6 week field visits i.e. prior to measurement (e.g. Riechelmann et al., 2013). To assess this, instantaneous in situ measurements of dripwater pH using micro-electrodes, were compared with pH measured (using the same electrodes) in the water accumulated over the previous 36 days in our regular collection vessels. We performed this experiment at our high and low-flow sites during September 2008. At our high-flow site, the accumulated sample was 0.2 pH units higher than the instantaneous measurement of 7.98 (which rose 0.02–0.03 after each drip before re-settling to 7.98 prior to the next drip). By contrast, instantaneous pH measurements were identical to those from the accumulated sample at our low-flow site (8.15). This is consistent with our observations of minimal calcite deposition on our collection vessels at our low-flow site versus significant calcite deposition on our high-flow vessel. This implies that our dripwater PCO_2 and SIcc calculations for our high-flow site may be under-estimated although we expect that the impact on our low-flow site is minimal. In the following section, we quantitatively investigate the impact of PCP on our dripwaters and assess where PCP is occurring in our system. We highlight that with our reverse modelling approach, any degassing prior to pH measurement is corrected in our first experiment and any calcite precipitation in the vessel is also corrected in our second experiment.

Dripwater Mg concentrations are also shown (Fig. 2) and contain a long-term rise of approximately 1–2 mg l^{-1} from 2006 to 2014 CE, although there are shorter-term variations between sites. We comment further on this trend in section 5.3, but reserve a more complete examination of Mg and other dripwater solutes, to a forthcoming paper.

4.3. PCP signal in dripwaters

The seasonal cycle in Ca and alkalinity concentrations suggests a PCP mechanism i.e. loss of Ca. This is confirmed by comparing the ln(Sr/Ca) vs ln(Mg/Ca) slopes of our dripwater data (0.95–1.00) with the calculated PCP trendlines which have slopes of 0.92, shown for sites 1A, 2E and 2A in Fig. 4. In this case, the slope of a PCP trendline is a function of the partition coefficients used. For example, re-calculating this trendline for site 2A using $K_{Sr} = 0.05$ rather than 0.1, brings this slope into agreement with that of site 2A dripwater data (0.97; in Fig. 4). These values also compare favourably with the theoretical value derived by Sinclair et al. (2012) to diagnose water/rock interactions such as PCP (0.88 ± 0.13).

From Fig. 4, we can interpret that the high-flow site, 2E, appears to have been impacted least by PCP indicated by data plotting to the lower left corner of the ln(Mg/Ca) versus ln(Sr/Ca plot. Additionally, Fig. 4 suggests that the dripwater infiltrating sites 1A and 1B, was originally derived from fluid with higher Sr/Ca.

5. Discussion

In the following sections, we further investigate the PCP history of the dripwaters and the implications for speleothem records from Golgotha Cave. In section 5.1 we investigate whether the contrasting behaviour between low and high-flow sites can be entirely explained by the PCP process, or require differences in dripwater composition since our previous study confirmed that our high-flow site derives water from a distinct store (Treble et al., 2013). By restoring these solutions to their composition when they were originally in equilibrium with limestone, we can quantify the impact of PCP and also examine whether or not there is a long-term evolution of the carbonate system over our period of monitoring. In section 5.2, we discuss where PCP is occurring in the flowpath and the relationship between PCP and stalactite drip rate. In section 5.3, we discuss the implications of our findings for stalagmite trace element records and forward model the predicted Mg/Ca values for the underlying stalagmite at our low-flow site.

5.1. Modelling of dripwater flowpath history

Most of our dripwaters are supersaturated with respect to calcite, a condition that requires degassing of CO_2 from a solution

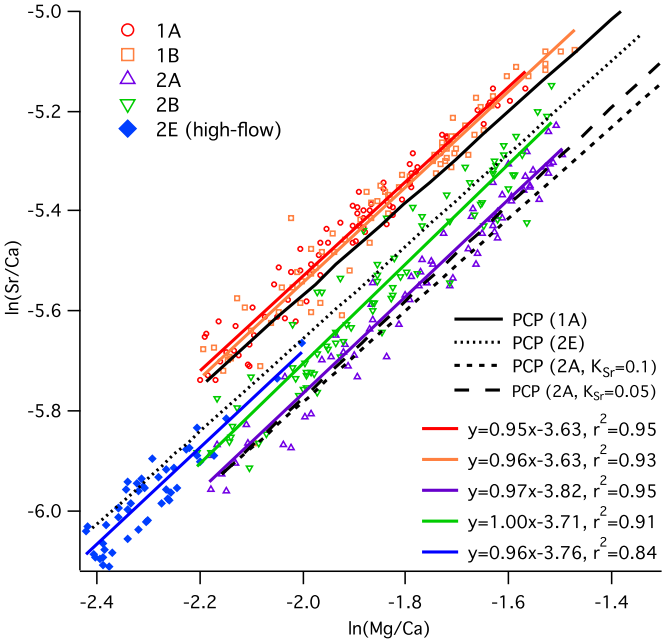

Fig. 4. Dripwater ln(Sr/Ca) versus ln(Mg/Ca) (weight ratio) data, with linear fits for each site, plus calculated PCP trendlines for sites 1A, 2E and 2A. PCP trendline for site 2A is shown twice, using $K_{Sr} = 0.1$ and $K_{Sr} = 0.05$, see text in section 4.3. See Methods for PCP trendline calculation.

that had previously been in equilibrium with limestone. Our Mg/Ca to Sr/Ca relationship (Fig. 4) also indicates that at least some dripwaters have experienced PCP. In order to estimate the original concentration of ions equilibrated with our host rock, we conducted two reverse modelling experiments using our contrasting solutions (site 1A: low-flow and site 2E: high-flow). Model experiment 1 involves returning the solution to calcite saturation by simple addition of CO_2, thus simulating the consequence of degassing as the sole process for modifying solution chemistry. Model experiment 2 reverses the effects both of degassing and of calcite precipitation in order to yield a solution, in equilibrium with calcite, with Mg/Ca equal to the minimum value for each site (see Section 3.3). Since calcite precipitation is stoichiometric, the Ca required to restore Mg/Ca to the lowest value in the series is used to calculate the required $CaCO_3$ addition, and speciation software is then used to calculate the CO_2 addition required to restore the solution to equilibrium at this low Mg/Ca value.

Our reverse modelled dripwater PCO_2 values for our high and low-flow dripwaters are compared with the measured dripwater and cave PCO_2 in Fig. 5. For both sites, our modelled undegassed PCO_2 values (experiment 1) are similar to those measured when cave PCO_2 is high, suggesting that our dripwaters are in equilibrium with cave CO_2 during high CO_2 mode. A few points result in measured dripwater PCO_2 which was higher than modelled (e.g. February, October and November 2010; Fig. 5) indicating that they were undersaturated at the time of measurement. This implies open-system dissolution conditions with the dissolution of aqueous CO_2 having outpaced dissolution of $CaCO_3$ at some point above the cave in these cases. This could be attributed to build-up of CO_2 within the host rock and insufficient dissolution time and/or availability of $CaCO_3$ near the cave roof to maintain calcite saturation. Similarly, a build-up of CO_2 could explain transient maxima in dissolved Ca associated with the summer high PCO_2 for site 2E in recent years (Fig. 2) if dripwaters associated with this site were able to access and dissolve host-rock calcite.

Modelled (undegassed) dripwater PCO_2 show a clear reduction in seasonality for our high-flow data but not for our low-flow site (Fig. 5). This suggests that the annual cycle in our measured high-flow dripwater PCO_2 is driven simply by equilibration with the cave atmosphere (i.e. degassing) whilst that in our low-flow dripwater may be dominated by an additional process (e.g. PCP). This was confirmed by model experiment 2 which involved reverse modelling the composition of waters before they experienced PCP. This resulted in a further reduction in PCO_2 seasonality, particularly for our low-flow site, when dripwaters were restored to their minimum Mg/Ca values (0.111 for low-flow; 0.0887 for high-flow) representing a minimum estimate of the highest PCO_2 that the waters had encountered. These PCO_2 values are $10^{-2.43}$ to $10^{-2.11}$ for the low-flow site and $10^{-2.17}$ to $10^{-1.90}$ for the high-flow site. However, if our low-flow waters were also restored to the high-flow minimum Mg/Ca value of 0.0887, higher PCO_2 values with an identical mean to the high-flow drip calculation are found, implying that both waters originally equilibrated at similar CO_2 concentrations. This suggests that the variability in SI_{cc} between our low and high-flow sites (Fig. 2) is driven by PCP rather than the alternative possibility of contrasting initial solution chemistries.

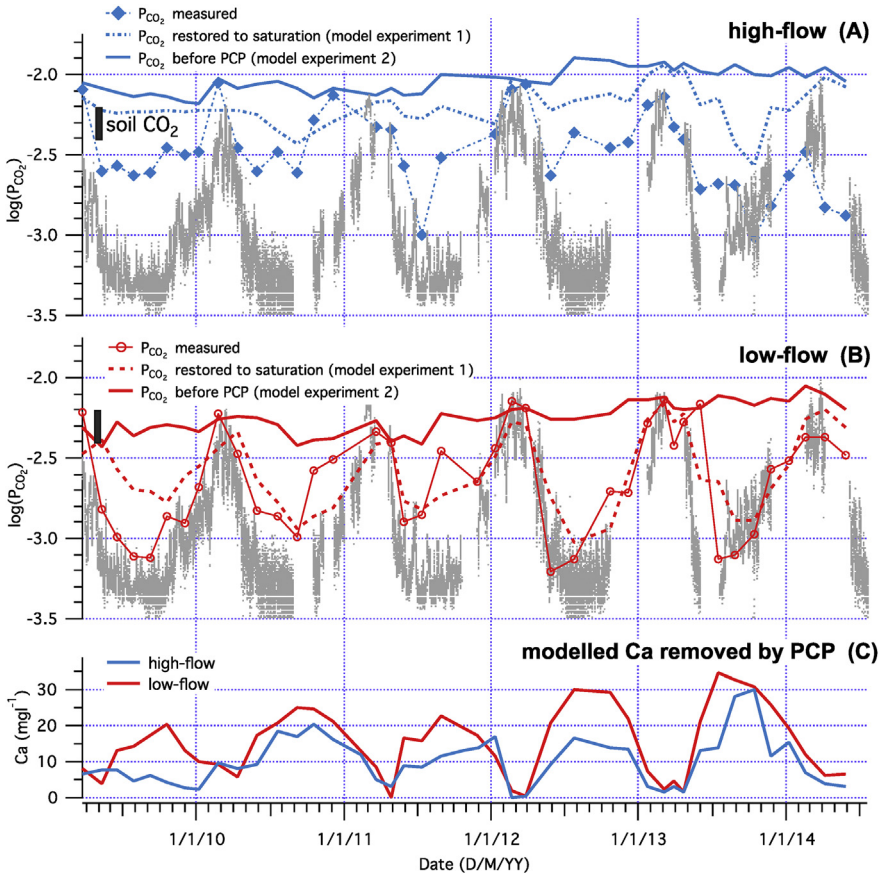

Fig. 5. A–C: A comparison between measured and modelled dripwater PCO_2 values for our high-flow site (A); and our low-flow site (B). The calculated amounts of Ca precipitated from solution via PCP are also shown (C). Grey dots are our in situ measured cave air PCO_2 data. Black vertical bar indicates range of soil CO_2 measurements. Model experiment 1 restores dripwater PCO_2 to saturation with respect to calcite (i.e. undegassed values) and model experiment 2 reverse-models the PCP process on the undegassed waters.

We argue that our modelling has also shown that the greater impact of PCP at our low-flow site is a function of drip rate, discussed further below.

Our modelling demonstrates that high-flow dripwater PCO_2 data primarily responds to equilibration with the cave atmosphere whilst low-flow dripwater PCO_2 data are additionally, and significantly, impacted by PCP. Both processes are comparatively suppressed during high CO_2 mode when reduced ventilation raises cave air PCO_2 to the point that it is in equilibrium with its original source CO_2 from the unsaturated zone. By contrast when Golgotha Cave ventilates, lowering cave air PCO_2, dripwaters equilibrate to cave PCO_2, producing seasonal minima in dripwater PCO_2 at both high and low-flow sites, but with further progression to in-cave PCP at our low-flow site where drip rates are sufficiently long for PCP to occur and affect stalactite water. The relationship between drip rate and PCP in Golgotha Cave is further evident by the >20% decrease in mean dripwater Ca, indicating enhanced PCP, following the reduction in drip intervals from approximately 1 to 5 min in February 2007 at site 2B (Fig. 2).

Our values obtained from restoring the original chemistry of the source water via our reverse modelling experiments are: i) much higher, at least for our high-flow site, than our shallow measurements (0.2–0.5 m) of soil PCO_2 ($10^{-2.4}$ to $10^{-2.2}$); and ii) lack seasonality (Fig. 5). This implies that our dripwaters encounter a relatively deep source of CO_2 and this helps to explain seasonally undersaturated waters also. This result is consistent with tree roots, injecting CO_2 into the deeper unsaturated zone (cf. Meyer et al., 2014) or the presence of sufficient vadoze zone microbial respiration to generate significant CO_2 there (cf. ground air CO_2, Atkinson, 1977). A rise in CO_2 concentrations in the vadose zone owing to these processes is not uncommon (Langmuir, 1997). For example, Wood et al. (2014) measured the soil CO_2 in five vadose zone profiles in central Australia. In the top 5 m of each profile, CO_2 concentrations were less than 10,000 ppmv, while CO_2 concentrations increased to 20,000–30,000 ppmv at 10–15 m below the ground surface.

Further consideration of our reverse-modelled PCO_2 for high versus low-flow data, indicates that both show an overall rising parallel trend, implying rising concentrations of our CO_2 source between 2009 and 2013 CE, consistent with the measured rise in cave PCO_2 during high-CO_2 mode over the same interval (Fig. 5). We suggest that this rising trend may be capturing the long-term effects of the recovery from fires that impacted this site in 2006 CE, given the time required for forest regrowth and for root respiration to revert to previous maximum levels (Coleborn et al., in review).

Finally, the small reversal of this rising CO_2 trend at our high-flow site (2E) during the relatively wetter year 2013 (Fig. 5) may be highlighting a possible non-linear anomaly to the typical recharge-PCP relationship (e.g. McDonald et al., 2004; Tremaine and Froelich, 2013; Karmann et al., 2007). That is, our dripwater measurements show an example of enhanced PCP during a period of higher rainfall. We propose a possible scenario of higher infiltration during 2013 filling the preferential flow store that feeds this site (see Treble et al., 2013), trapping air below a zone of high saturation resulting in enhanced PCP, indicated by model experiment 1 data (Fig. 5). Additionally, the fact that the reverse-modelled fluid PCO_2 starts to decline indicates that this higher infiltration may also have: i) inhibited downwards diffusion of CO_2, or ii) inhibited vadose-zone microbial CO_2-production as local anoxia occurs.

5.2. Relationship between PCP and drip rate

Our modelling shows that the extent of PCP at Golgotha Cave is primarily determined by drip rate. That is, water dripping from our high-flow site does not always have time to fully equilibrate with the cave atmosphere, and thus significant PCP does not occur before falling from the stalactite. We attribute greater PCP at our low-flow sites to stalactite deposition. Long (0.1–1 m) stalactites are common above site 1 whilst minimal stalactite growth occurs above site 2 where drip rates are higher.

We have identified that PCP becomes dominant at drip intervals longer than those measured at site 2E (30 s). Small (~10%) variations in 2E drip rate (Fig. 5) appear to influence degassing of unsaturated waters, but are insufficient to impact PCP (cf. Hansen et al., 2013). Thus the threshold for enhanced stalactite precipitation in Golgotha Cave probably lies between 30 s and 60 s; the latter being the drip interval at site 2B prior to February 2007, during which drip water PCO_2 is the same as other low-flow sites (Fig. 2). This interval compares well to our understanding of the rate-determining steps during speleothem formation (Dreybrodt and Scholz, 2011; Hansen et al., 2013).

Interestingly, the influence of PCP on a particular drip site could become significant if drip rates cross this threshold, since stalactite formation is a balance between water supply and equilibration time. This has important implications for interpreting the underlying stalagmite record since the magnitude of PCP directly varies with the duration of the drip interval above this threshold. We discuss this further and examine the implications for the stalagmite record in Sections 5.3–5.4.

The influence of drip rate on PCP is discussed in other cave studies (Tooth and Fairchild, 2003; McDonald et al., 2007; Mattey et al., 2010; Riechelmann et al., 2011; Wong et al., 2011; Stoll et al., 2012). However, our data offer the clearest evidence of this relationship which we argue can be attributed to features arising from the relatively simple hydrogeology of Golgotha Cave. That is: i) PCP is predominantly isolated on the tips of soda-straw stalactites rather the additional complication of PCP along the flowpath; and ii) we are able to compare high and low-flow sites whose drip intervals are relatively temporally consistent, but whose mean values vary by an order of magnitude making this relationship clearer to identify. We emphasize that it is the hydrogeology of Golgotha Cave (specifically the predominance of matrix-flow) that allows us to highlight these geochemical processes which are masked at sites with more complex hydrogeology. Additionally, from our field observations, it appeared that water flowed down the interior of all soda-straw stalactites feeding our sites (with the possible exception of site 2B), limiting the opportunity for CO_2 degassing until water reaches the stalactite tip. Water flowing down the exterior of stalactites may promote additional PCP.

5.3. Implications of PCP for speleothem records from Golgotha Cave

The relationship between PCP and drip interval provides important distinctions in interpreting Mg and Sr trace element records from speleothems at our high versus low-flow sites and we have summarized this in the conceptual model below (Fig. 6). Long drip intervals promote PCP on the stalactite tips at our low-flow sites, hence (ventilation-driven) in-cave PCP will be the dominant mechanism driving dripwater Mg/Ca and Sr/Ca at our low-flow sites and we model how this may appear in Section 5.4. At much shorter drip intervals, there is less time for stalactite water to equilibrate, resulting in less evolved solutions at our high-flow sites. Hence our high-flow sites are relatively insensitive to PCP and as a consequence, along-axis measurements of stalagmites from these sites may preserve concentrations of trace elements from the unsaturated-zone waters. Hence, an important outcome of this study is that trace elements from these stalagmites potentially provide environmental information on changing biogeochemical fluxes of these ions; i.e. associated with variations in aerosol flux, bedrock dissolution, forest bioproductivity etc. Stalagmite Mg and

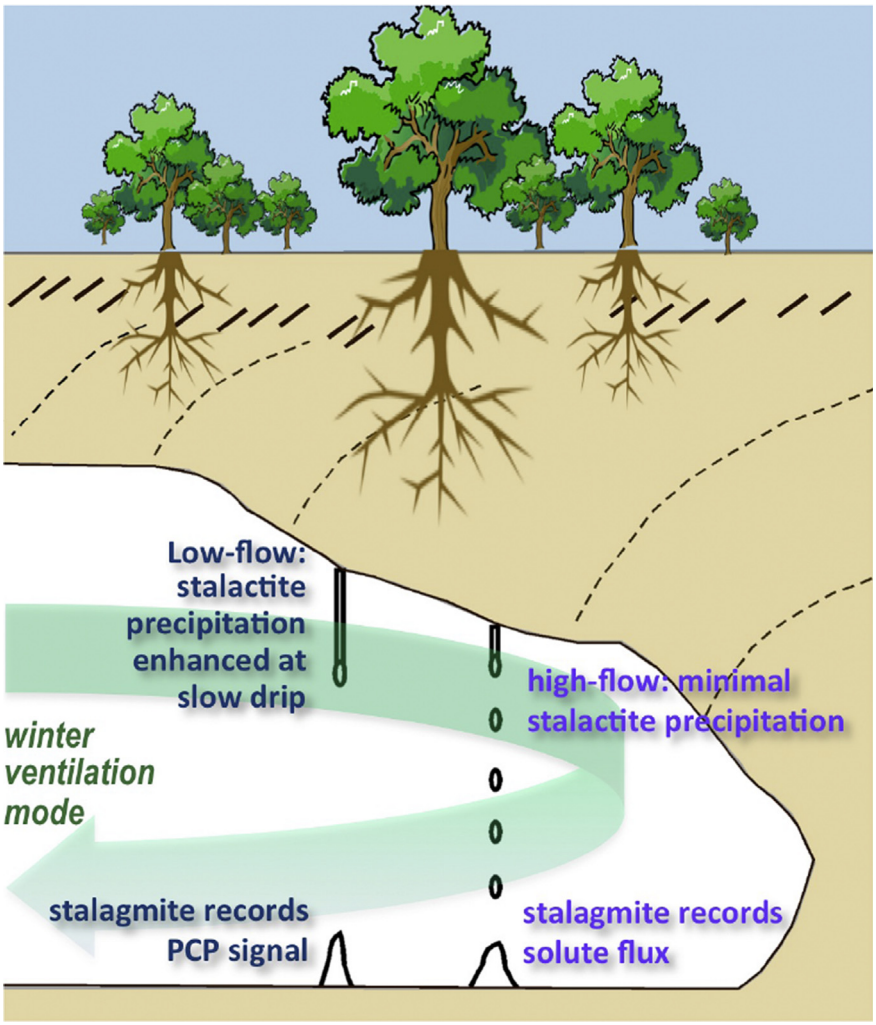

Fig. 6. Conceptual model illustrating the implications of in-cave or stalactite PCP during winter ventilation mode. Stalactite precipitation is enhanced by PCP during longer drip intervals at our low-flow sites and may likely be the dominant signal in stalagmite Mg/Ca and Sr/Ca records from these sites. Shorter-drip intervals at our high-flow site minimise stalactite PCP. Stalagmite Mg/Ca and Sr/Ca records from our high-flow sites have greater potential to preserve environmental information from dripwater Mg, Sr and/or other PCP-sensitive ion fluxes.

Sr records from our high-flow site could be interpreted in this way. The specific processes relevant to our dripwater dataset and the environmental significance of their long-term trends are investigated in detail in a forthcoming article.

5.4. Forward modelling the PCP signal in speleothems from our low-flow sites

Long-term trends in dripwater chemistry are unlikely to be preserved in speleothems from low-flow sites if these signals are smaller than that imparted by the in-cave PCP process. To investigate how dominant this signal is and whether the PCP signal may itself offer a useful environmental proxy, we forward modelled the dripwater from our low-flow site (1A) to calculate the Mg/Ca composition of the resultant fluid that had degassed to equilibrium with cave air and had reached equilibrium between water and $CaCO_3$ (i.e. speleothem-precipitating fluid). Fig. 7 shows this modelled fluid, our measured dripwater Mg/Ca and measured cave $\log(PCO_2)$ for site 1A. Shown also for comparison are the final Mg/Ca ratio measured on the stalagmite collected underneath drip site 1A immediately prior to this monitoring commencing (unpublished data). This stalagmite Mg/Ca value is converted to a fluid Mg/Ca value for comparison, using K_{Mg}. The close agreement between stalagmite and the modelled fluid values (Fig. 7) demonstrates that our modelled equilibrated fluid Mg/Ca values are realistic for our low-flow site. This further supports that water dripping from our low-flow stalactite is already close to equilibration.

Fig. 7 shows a rising trend in modelled fluid Mg/Ca maxima. The highest values in mid-2013 (Mg/Ca = 0.28) correspond to a coincidence between ventilated cave air conditions and epikarst PCO_2 that had reached its maximum value (Fig. 7) producing the strongest CO_2 gradient between the original equilibrated chemistry and the cave air, maximising PCP. Under these conditions, modelled fluid Mg/Ca was three times higher than its inferred value before PCP (0.11). Hence, the PCP process is the dominant signal in our stalagmite from low-flow sites particularly since our SI_{cc} data show that stalagmites from our low-flow sites will be biased towards precipitation during the cooler months. For example, the PCP process would dominate smaller magnitude signals such as the long-term rise in Mg concentrations observed in our dripwater (Fig. 2) equivalent to a difference in Mg/Ca values of <0.05.

Thus in stalagmites from our low-flow sites, we would expect Mg/Ca (and Sr/Ca as well as other PCP-sensitive ions) to act as a proxy for changes in the CO_2 gradient between source and cave,

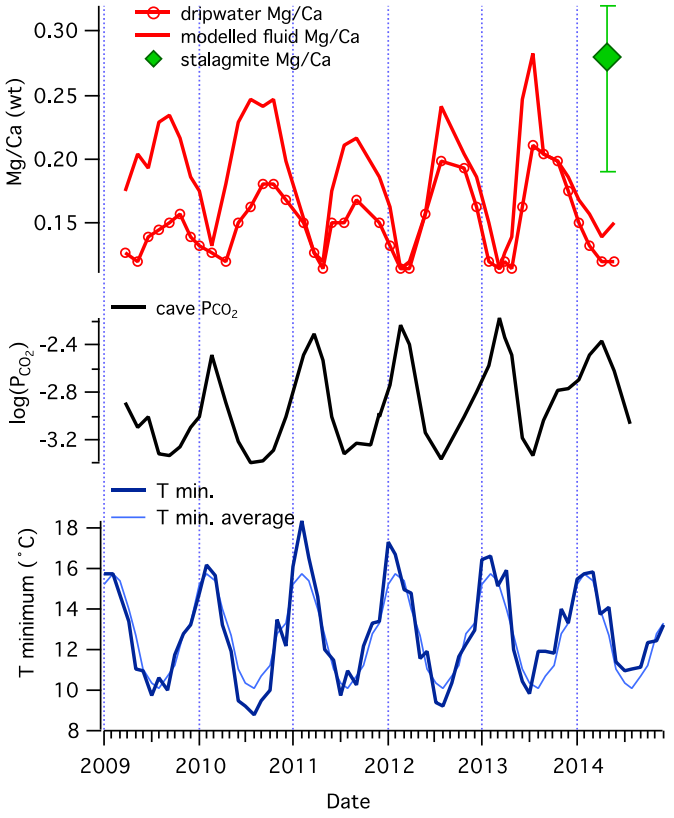

Fig. 7. Forward modelled fluid Mg/Ca compared with dripwater Mg/Ca, cave air PCO_2 and minimum temperature (expressed as monthly mean of daily minimums) for our low-flow site (site 1A). The Mg/Ca ratio measured on the top of the stalagmite collected underneath this drip site is also shown. This value is converted to the equivalent in fluid Mg/Ca for comparison and is bracketed by the range of values measured within the upper 1.5 mm of calcite, estimated to have precipitated within the last two decades, although our age model for this stalagmite is incomplete. Our forward-modelled fluid Mg/Ca represent maximum values when equilibrium is fully attained. Thus similar values would arise if we forward-modelled our high-flow data since our reverse-modelling showed that both solutions initially equilibrated with similar PCO_2 values. In practice, for our high-flow site, this end-member may represent cave pools at the end of the flowline. Comparison of stalagmite crest and flanks can indicate how close to the end-member a particular stalagmite has reached.

either via changes in the source CO_2 concentration or cave ventilation. The impacts of cave ventilation will potentially be detectable in high-resolution measurements (sub-seasonal). For example, our high Mg/Ca values rapidly decrease between July and August 2013, several months earlier than in previous years (Fig. 7). This is in response to the early transition to non-ventilated mode initiated by outside air temperatures that were ~2 °C warmer than usual.

As an aside, we could draw from this that the strong inverse relationship between speleothem Mg/Ca and cave CO_2 (Fig. 7) raises the potential for sub-seasonal measurements of speleothem Mg to be used as a proxy for external temperature information (cf. Wynn et al., 2014), especially since buoyancy-driven cave ventilation can potentially be modelled as a physical process (Linden, 1999; Gregorič et al., 2011). This potentially could be applied to very high-resolution speleothem data to investigate anomalies in cool-season duration (e.g. our example given above). Such anomalies would be relative to the average temperature over a timescale set by the cave temperature equilibration time.

6. Conclusions

The modification of infiltrating water from the surface to the stalagmite is particularly straightforward to isolate at Golgotha Cave because of its relatively simple hydrogeology, i.e. the predominance of matrix flowpaths and insignificant PCP above the cave ceiling minimises the complexity of the karst architecture on the hydrogeochemical signals in the dripwater. Our data-model comparison has shown that in-cave PCP at the stalactite tip dominates PCP-sensitive ions in our low-flow dripwaters during winter ventilation mode. As the dripwaters from our low-flow sites become sufficiently saturated only during the ventilated mode, this PCP signal will be enhanced in the underlying stalagmites. We have identified that this process becomes dominant at drip intervals longer than 30 s and have modelled that the PCP process could overprint other geochemical signals transmitted from the surface environment into the underlying stalagmite.

Importantly, we interpret from these findings that stalagmites formed under variable drip rates could cross such a threshold, altering both the potential seasonal growth bias as well as their sensitivity to PCP. In theory, this could result in a stalagmite record that contains multiple periods where PCP is insignificant (trace element concentrations driven by biogeochemical fluxes) as well as periods where PCP is significant (sufficient to dominate other signals). Stalagmite morphology, crystal fabric and a well-constructed chronology could be used to detect growth rate changes (e.g. Frisia et al., 2000; Baldini, 2001; Miorandi et al., 2010) and be used to identify the potential for such problems.

Our study has quantified the impacts of PCP on our dripwaters and specifically highlighted the role of in-cave PCP, which is enhanced on stalactites in the case of longer drip intervals. This finding is relevant for all cave systems and should be considered when interpreting stalagmite records from low or variable-flow drips. There will be some variability around the identified threshold of drip rates between 30 and 60 s, since soda-straw stalactites (this study) yield have water that is not fully degassed, whereas solid stalactites are likely to drip fully degassed water.

Finally, our restored initial solutions suggest a long-term rise in CO_2 in the unsaturated zone, which we attribute to the recovery of forest growth following fires. Complementary evidence for this hypothesis will be shown in a forthcoming article that examines the trends in dripwater solutes. The future investigation of these dripwater solutes will inform the interpretation of speleothem trace elements from our high-flow site which will more likely preserve environmental signals from the unsaturated zone, rather than be dominated by the PCP effects demonstrated in this paper.

Acknowledgements

We gratefully acknowledge and thank the following people for their assistance with fieldwork and sample analyses: Monika Markowska, Robert Baker and the staff of Calgardup Cave, Ursula Salmon, Henri Wong, Stuart Hankin, Chris Waring, Suan Wong, Paul Rustomji, Warren Bond, Carol Tadros and Dan Gregg. We also thank the WA Department of Parks and Wildlife for fire history information and Anne Ankcorn for cartography. PCT acknowledges the support of a Land & Water Australia grant (project number ANU52) and laboratory facilities at the Australian Nuclear Science and Technology Organisation and the Australian National University. The Golgotha Cave maps were reproduced in modified form with permission from Barry Loveday's 1997 survey. Some ideas for this study were generated from ARC Linkage Project LP130100177 awarded to AB, IJF and PCT and the outcomes of this study contribute to ARC Discovery Project DP140102059 awarded to PCT.

References

Atkinson, T.C., 1977. Carbon-dioxide in atmosphere of unsaturated zone – important control of groundwater hardness in limestones. J. Hydrol. 35, 111–123.

Baker, A., Genty, D., Fairchild, I.J., 2000. Hydrological characterisation of stalagmite drip waters at Grotte de Villars, Dordogne, by the analysis of inorganic species and luminescent organic matter. Hydrol. Earth Syst. Sci. 4, 439–450.

Baldini, J.U.L., 2001. Morphologic and dimensional linkage between recently deposited speleothems and dripwater from Browns Folly Mine, Wiltshire, England. J. Cave Karst Stud. 63, 83–90.

Baldini, J.U.L., McDermott, F., Fairchild, I.J., 2006. Spatial variability in cave drip water hydrochemistry: Implications for stalagmite paleoclimate records. Chem. Geol. 235, 390–404.

Baldini, L.M., McDermott, F., Baldini, J.U.L., Arias, P., Cueto, M., Fairchild, I.J., Hoffmann, D.L., Mattey, D.P., Müller, W., Constantin Nita, D., Ontañon, R., Garciá-Moncó, C., Richards, D.A., 2015. Rapid repositioning of North Atlantic atmospheric circulation during the Younger Dryas Event. Earth Planet. Sci. Lett. 419, 101–110.

Bureau of Meteorology, 2014. Climate Statistics. http://www.bom.gov.au/climate/data/ (accessed 15.01.14.).

Coleborn, K., Spate, A., Tozer, M., Andersen, M.S., Fairchild, I.J., MacKenzie, B., Treble, P.C., Meehan, S., Baker, A., Baker, A., 2015. Effects of wildfire on long-term soil CO_2 concentration: implications for karst processes. Environ. Earth Sci. (submitted for publication).

Cruz, F.W., Burns, S.J., Jercinovic, M., Karmann, I., Sharp, W.D., Vuille, M., 2007. Evidence of rainfall variations in Southern Brazil from trace element ratios (Mg/Ca and Sr/Ca) in a Late Pleistocene stalagmite. Geochim. Cosmochim. Acta 71, 2250–2263.

Day, C.C., Henderson, G.M., 2013. Controls on trace-element partitioning in cave-analogue calcite. Geochimica Cosmochim. Acta 120, 612–627.

DPaW (Department of Parks and Wildlife WA), 2012. Fire History Map: Calgardup Cave to Golgotha Cave. Kirup Fire Management Services. Generated 23/10/2012.

Dreybrodt, W., Scholz, D., 2011. Climatic dependence of stable carbon and oxygen isotope signals recorded in speleothems: from soil water to speleothem calcite. Geochimica Cosmochim. Acta 75, 734–752.

Fairchild, I.J., Baker, A., 2012. Speleothem Science: from Process to Past Environments. Wiley-Blackwell, Oxford.

Fairchild, I.J., Treble, P.C., 2009. Trace elements in speleothems as recorders of environmental change. Quat. Sci. Rev. 28, 449–468.

Fairchild, I.J., Borsato, A., Tooth, A.F., Frisia, S., Hawkesworth, C.J., Huang, Y., McDermott, F., Spiro, B., 2000. Controls on trace element (Sr-Mg) compositions of carbonate cave waters: implications for speleothem climatic records. Chem. Geol. 166, 255–269.

Fairchild, I.J., Smith, C.L., Baker, A., Fuller, L., Spötl, C., Mattey, D., McDermott, F., EIMF, 2006. Modification and preservation of environmental signals in speleothems. Earth Sci. Rev. 75, 105–153.

Frisia, S., Borsato, A., fairchild, I.J., McDermott, F., 2000. Calcite fabrics, growth mechanisms and environments of formation in speleothems (Italian Alps and SW Ireland). J. Sediment. Res. 70, 1183–1196.

Frisia, S., Borsato, A., Fairchild, I.J., Susini, J., 2005. Variations in atmospheric sulphate recorded in stalagmites by synchrotron micro-XRF and XANES analyses. Earth Planet. Sci. Lett. 235, 729–740.

Frisia, S., Fairchild, I.J., Fohlmeister, J., Miorandi, R., Spotl, C., Borsato, A., 2011. Carbon mass-balance modelling and carbon isotope exchange processes in dynamic caves. Geochimica Cosmochim. Acta 75, 380–400.

Gascoyne, M., 1983. Trace-element partition coefficients in the calcite-water system and their paleoclimatic significance in cave studies. J. Hydrol. 61, 213–222.

Goede, A., McCulloch, M., McDermott, F., Hawkesworth, C., 1998. Aeolian contribution to strontium and strontium isotope variations in a Tasmanian speleothem. Chem. Geol. 149, 37–50.

Genty, D., Deflandre, G., 1998. Drip flow variations under a stalactite of the Pere Noel cave (Belgium). Evidence of seasonal variations and air pressure constraints. J. Hydrol. 211, 208–232.

Gregorič, A., Zidanšek, A., Vaupotič, J., 2011. Dependence of radon levels in Postojna Cave on outside air temperature. Nat. Hazard. Earth Syst. Sci. 11, 1523–1528.

Hall, G.J., Marnham, J.R., 2002. Regolith-landform Resources of the Karridale-Tooker and Leeuwin 1:50000 Sheets. Dept. of Mineral and Petroleum Resources, Geologogical Survey of Western Australia, Perth, p. 74.

Hansen, M., Dreybrodt, W., Scholz, D., 2013. Chemical evolution of dissolved inorganic carbon species flowing in thin water films and its implications for (rapid) degassing of CO_2 during speleothem growth. Geochimica Cosmochim. Acta 107, 242–251.

Hartland, A., Fairchild, I.J., Lead, J.R., Borsato, A., Baker, A., Frisia, S., Baalousha, M., 2012. From soil to cave: transport of trace metals by natural organic matter in karst dripwaters. Chem. Geol. 304, 68–82.

Hori, M., Ishikawa, T., Nagaishi, K., You, C.F., Huang, K.F., Shen, C.C., Kano, A., 2014. Rare earth elements in a stalagmite from southwestern Japan: a potential proxy for chemical weathering. Geochem. J. 48, 73–84.

Huang, Y., Fairchild, I.J., 2001. Partitioning of Sr^{2+} and Mg^{2+} into calcite under karst-analogue experimental conditions. Geochimica Cosmochim. Acta 65, 47–62.

Johnson, K.R., Ingram, B.L., Sharp, W.D., Zhang, P.Z., 2006. East Asian summer monsoon variability during Marine Isotope Stage 5 based on speleothem delta O-18 records from Wanxiang Cave, central China. Palaeogeogr. Palaeoclimatol. Palaeoecol. 236, 5–19.

Kowalczk, A.J., Froelich, P.N., 2010. Cave air ventilation and CO_2 outgassing by radon-222 modeling: how fast do caves breathe? Earth Planet. Sci. Lett. 289, 209–219.

Karmann, I., Cruz, F., Viana, O., Burns, S., 2007. Climate influence on geochemistry parameters of waters from Santana-Perolas cave system, Brazil. Chem. Geol. 244, 232–247.

Lambert, W.J., Aharon, P., 2011. Controls on dissolved inorganic carbon and $\delta^{13}C$ in cave waters from DeSoto Caverns: implications for speleothem $\delta^{13}C$ assessments. Geochimica Cosmochim. Acta 75, 753–768.

Langmuir, D., 1997. Aqueous Environmental Geochemistry. Prentice Hall, New Jersey, p. 600.

Linden, P.F., 1999. The fluid mechanics of natural ventilation. Annu. Rev. fluid Mech. 31, 201–238.

Mahmud, K., Mariethoz, G., Treble, P.C., Baker, A., 2015. Lidar survey and geostatistical analysis to identify infiltration properties in the Tamala Limestone, Western Australia. IEEE J. Sel. Top. Appl. Earth Observ. Remote Sens. (submitted for publication).

Mattey, D.P., Fairchild, I.J., Atkinson, T.C., Latin, J.-P., Ainsworth, M., Durell, R., 2010. Seasonal microclimate ocntrol of calcite fabrics, stable isotopes and trace elements in modern speleothem from St Michaels Cave, Gibraltar. In: Pedley, H.M., Rogerson, M. (Eds.), Tufas and Speleothems: Unravelling the Microbial and Physical Controls, Geological Society, London, Special Publication, vol. 336, pp. 323–344.

McDonald, J., Drysdale, R., Hill, D., 2004. The 2002–2003 El Nino recorded in Australian cave drip waters:Implications for reconstructing rainfall histories using stalagmites. Geophys. Res. Lett. 31, L22202. http://dx.doi.org/10.1029/2004GL020859.

McDonald, J., Drysdale, R., Hill, D., Chisari, R., Wong, H., 2007. The hydrochemical response of cave drip waters to sub-annual and inter-annual climate variability, Wombeyan Caves, SE Australia. Chem. Geol. 244, 605–623.

McDonald, J., Drysdale, R.N., 2007. Hydrology of cave drip waters at varying bedrock depths from a karst system in southeastern Australia. Hydrol. Process. 21, 1737–1748.

McMillan, E.A., Fairchild, I.J., Frisia, S., Borsato, A., McDermott, F., 2005. Annual trace element cycles in calcite-aragonite speleothems: evidence of drought in the western Mediterranean 1200-1100 yr BP. J. Quat. Sci. 20, 423–433.

Meyer, K.W., Feng, W.M., Breecker, D.O., Banner, J.L., Guilfoyle, A., 2014. Interpretation of speleothem calcite delta C-13 variations: evidence from monitoring soil CO2, drip water, and modern speleothem calcite in central Texas. Geochimica Cosmochim. Acta 142, 281–298.

Miorandi, R., Borsato, A., Frisia, S., Fairchild, I., Richter, D., 2010. Epikarst hydrology and implications for stalagmite capture of climate changes at Grotta di Ernesto (NE Italy): results from long-term monitoring. Hydrol. Process. 34, 3101–3114.

Miotke, F.-D., 1974. Carbon dioxide and the soil atmosphere. Abhandl. Karst Höhlenk. A9, 1–49.

Musgrove, M., Banner, J.L., 2004. Controls on the spatial and temporal variability of vadose dripwater geochemistry: Edwards Aquifer, central Texas. Geochimica Cosmochim. Acta 68, 1007–1020.

Orland, I.J., Burstyn, Y., Bar-Matthews, M., Kozdon, R., Ayalon, A., Matthews, A., Valley, J.W., 2014. Seasonal climate signals (1990-2008) in a modern Soreq Cave stalagmite as revealed by high-resolution geochemical analysis. Chem. Geol. 363, 322–333.

Pape, J.R., Banner, J.L., Mack, L.E., Musgrove, M., Guilfoyle, A., 2010. Controls on oxygen isotope variability in precipitation and cave drip waters, central Texas, USA. J. Hydrol. 385, 203–215.

Parkhurst, D., Appelo, C., 1999. User's Guide to PHREEQC (Version 2) – a Computer Program for Speciation, Batch-reaction, One Dimensional Transport, and Inverse Geochemical Calculations. USGS Water Resources Investigations Report 99, p. 4259.

Raupach, M.R., Briggs, P.R., Haverd, V., King, E.A., Paget, M., Trudinger, C.M., 2009. Australian Water Availability Project (AWAP): CSIRO Marine and Atmospheric Research Component: Final Report for Phase 3. CAWCR Technical Report No. 013, p. 67.

Raupach, M.R., Briggs, P.R., Haverd, V., King, E.A., Paget, M., Trudinger, C.M., 2012. Australian Water Availability Project. CSIRO Marine and Atmospheric Research. Canberra, Australia. http://www.csiro.au/awap. Date of access 4/9/14.

Riechelmann, D.F.C., Schroder-Ritzrau, A., Scholz, D., Fohlmeister, J., Spotl, C., Richter, D.K., Mangini, A., 2011. Monitoring Bunker Cave (NW Germany): a prerequisite to interpret geochemical proxy data of speleothems from this site. J. Hydrol. 409, 682–695.

Riechelmann, D.F.C., Deininger, M., Scholz, D., Riechelmann, S., Schroder-Ritzrau, A., Spotl, C., Richter, D.K., Mangini, A., Immenhauser, A., 2013. Disequilibrium carbon and oxygen isotope fractionation in recent cave calcite: comparison of cave precipitates and model data. Geochimica Cosmochim. Acta 103, 232–244.

Rutlidge, H., Baker, A., Marjo, C.E., Andersen, M.S., Graham, P.W., Cuthbert, M.O., Rau, G.C., Roshan, H., Markowska, M., Mariethoz, G., Jex, C.N., 2014. Dripwater organic matter and trace element geochemistry in a semi-arid karst environment: Implications for speleothem paleoclimatology. Geochimica Cosmochim. Acta 135, 217–230.

Sinclair, D.J., Banner, J.L., Taylor, F.W., Partin, J., Jenson, J., Mylroie, J., Goddard, E., Quinn, T., Jocson, J., Miklavic, B., 2012. Magnesium and strontium systematics in tropical speleothems from the Western Pacific. Chem. Geol. 294, 1–17.

Spötl, C., Fairchild, I.J., Tooth, A.F., 2005. Cave air control on dripwater geochemistry, Obir Caves (Austria): implications for speleothem deposition in dynamically ventilated caves. Geochimica Cosmochim. Acta 69, 2451–2468.

Stoll, H.M., Muller, W., Prieto, M., 2012. I-STAL, a model for interpretation of Mg/Ca, Sr/Ca and Ba/Ca variations in speleothems and its forward and inverse application on seasonal to millennial scales. Geochem. Geophys. Geosyst. 13, Q09004. http://dx.doi.org/10.1029/2012GC004183.

Tooth, A.F., Fairchild, I.J., 2003. Soil and karst aquifer hydrological controls on the geochemical evolution of speleothem-forming drip waters, Crag Cave, southwest Ireland. J. Hydrol. 273, 51–68.

Treble, P., Shelley, J.M.G., Chappell, J., 2003. Comparison of high resolution sub-annual records of trace elements in a modern (1911-1992) speleothem with instrumental climate data from southwest Australia. Earth Planet. Sci. Lett. 216, 141–153.

Treble, P.C., Bradley, C., Wood, A., Baker, A., Jex, C.N., Fairchild, I.J., Gagan, M.K., Cowley, J., Azcurra, C., 2013. An isotopic and modelling study of flow paths and storage in Quaternary aeolinite, SW Australia: implications for speleothem paleoclimate records. Quat. Sci. Rev. 64, 90–103.

Tremaine, D.M., Froelich, P.N., 2013. Speleothem trace element signatures: a hydrologic geochemical study of modern cave dripwaters and farmed calcite. Geochimica Cosmochim. Acta 121, 522–545.

Wood, C., Cook, P.G., Harrington, G.A., Meredith, K., Kipfer, R., 2014. Factors affecting carbon-14 activity of unsaturated zone CO_2 and implications for groundwater dating. J. Hydrol. 519, 465–475.

Wong, C.I., Banner, J.L., Musgrove, M., 2011. Seasonal dripwater Mg/Ca and Sr/Ca variations driven by cave ventilation: implications for and modeling of speleothem paleoclimate records. Geochim. Cosmochim. Acta 75, 3514–3529.

Wynn, P.M., Borsato, A., Baker, A., Frisia, S., Miorandi, R., Fairchild, I.J., 2013. Biogeochemical cycling of sulphur in karst and transfer into speleothem archives at Grotta di Ernesto, Italy. Biogeochemistry 114, 255–267.

Wynn, P.M., Fairchild, I.J., Spotl, C., Hartland, A., Mattey, D., Fayard, B., Cotte, M., 2014. Synchrotron X-ray distinction of seasonal hydrological and temperature patterns in speleothem carbonate. Environ. Chem. 11, 28–36.